



THIS MANUSCRIPT HAS BEEN SUBMITTED TO THE JOURNAL OF GLACIOLOGY AND HAS NOT BEEN PEER-REVIEWED.

A Multi-year Analysis of Supraglacial Lake Seasonal Dynamics in the Karakoram

Journal:	<i>Journal of Glaciology</i>
Manuscript ID	JOG-2026-0019
Manuscript Type:	Article
Date Submitted by the Author:	07-Feb-2026
Complete List of Authors:	Khan, Imran; University of New Hampshire, Civil and Environmental Engineering; University of New Hampshire Institute for the Study of Earth Oceans and Space, Earth Systems Research Center Moradi, Mahsa; University of New Hampshire, Civil and Environmental Engineering; University of New Hampshire Institute for the Study of Earth Oceans and Space, Earth Systems Research Center Jacobs, Jennifer; University of New Hampshire, Department of Civil and Environmental Engineering; University of New Hampshire Institute for the Study of Earth Oceans and Space, Earth Systems Research Center Licciardi, Joseph; University of New Hampshire, Department of Earth Sciences
Keywords:	Debris-covered glaciers, Glacier hydrology, Glacier hazards
Abstract:	Supraglacial lakes are a key feature of many debris-covered glaciers in the Karakoram region. These lakes are highly dynamic, often forming and draining rapidly on seasonal timescales. However, due to their small size and transient nature, they are largely absent from regional and global glacial lake inventories. In this study, we used Sentinel-1 synthetic aperture radar (SAR) imagery to examine the seasonal (May to September) and interannual (2017 to 2023) dynamics of supraglacial lakes across six glaciers in the Karakoram at scales from 0.001 to 0.50 km ² . Our results show that small (<0.01 km ²) and ephemeral lakes dominate in number, with lake occurrence decreasing sharply as size increases. The lakes had a consistent seasonal pattern, with lake

	<p>numbers and cumulative area peaking early in the melt season (May or June). Lake formation was concentrated on nearly stagnant glacier surfaces characterized by a debris thickness of less than 0.5 m and a surface slope of less than 9 degrees. This study provides new insights into supraglacial lake dynamics across the Karakoram by quantifying their prevalence, seasonality, and surface controls. These findings are important for evaluating potential downstream hydrologic and hazard impacts and improving our understanding of glacier hydrology and melt processes.</p>

SCHOLARONE™
Manuscripts

A Multi-year Analysis of Supraglacial Lake Seasonal Dynamics in the Karakoram

1 **Imran Khan^{1,2*}, Mahsa Moradi^{1,2}, Jennifer M. Jacobs^{1,2}, Joseph M. Licciardi³**

2 ¹Department of Civil and Environmental Engineering, University of New Hampshire, Durham,
3 NH 03824, USA

4 ²Earth Systems Research Center, Institute for the Study of Earth, Oceans, and Space, University
5 of New Hampshire, Durham, NH 03824, USA

6 ³Department of Earth Sciences, University of New Hampshire, Durham, NH 03824, USA

7 * **Correspondence:** Imran Khan <imran.khan@unh.edu>

8 **Abstract**

9 Supraglacial lakes are a key feature of many debris-covered glaciers in the Karakoram region.
10 These lakes are highly dynamic, often forming and draining rapidly on seasonal timescales.
11 However, due to their small size and transient nature, they are largely absent from regional and
12 global glacial lake inventories. In this study, we used Sentinel-1 synthetic aperture radar (SAR)
13 imagery to examine the seasonal (May to September) and interannual (2017 to 2023) dynamics of
14 supraglacial lakes across six glaciers in the Karakoram at scales from 0.001 to 0.50 km². Our
15 results show that small (<0.01 km²) and ephemeral lakes dominate in number, with lake occurrence
16 decreasing sharply as size increases. The lakes had a consistent seasonal pattern, with lake numbers
17 and cumulative area peaking early in the melt season (May or June). Lake formation was
18 concentrated on nearly stagnant glacier surfaces characterized by a debris thickness of less than
19 0.5 m and a surface slope of less than 9 degrees. This study provides new insights into supraglacial
20 lake dynamics across the Karakoram by quantifying their prevalence, seasonality, and surface
21 controls. These findings are important for evaluating potential downstream hydrologic and hazard
22 impacts and improving our understanding of glacier hydrology and melt processes.

23 1. Introduction

24 The Karakoram is characterized by its steep topography, high mountains, and numerous dynamic
25 glaciers (Mölg et al. 2018; Farinotti et al. 2020). This mountain range is home to more than 13,000
26 glaciers, covering an area of approximately 22,800 km², and includes some of the largest glaciers
27 (>50 km long) outside of the polar regions (RGI Consortium 2017; Wendleder et al. 2018; Xie et
28 al. 2023). These glaciers are found at altitudes ranging from 2,300 to 8,600 m above sea level,
29 while most of the ice reserves are concentrated between 4,000 to 5,500 m (Copland et al. 2011;
30 Hewitt 2011; Mölg et al. 2018). The steep mountain walls in the Karakoram are prone to frequent
31 rockfalls and avalanches, which deliver extensive debris that covers the ablation zones of many
32 glaciers in the region (Xie et al. 2023). This thick debris cover insulates the glacier and reduces
33 melt rates, a phenomenon that, along with favorable meteorological conditions, is suggested to be
34 a driving factor of the Karakoram Anomaly (Bisset et al. 2020; Zhu et al. 2024). The Karakoram
35 Anomaly refers to the observed stability or slight mass gain of glaciers in the Karakoram region
36 in contrast to widespread glacier retreat across the rest of the Himalaya (Farinotti et al. 2020).

37 A key feature of several of Karakoram's debris-covered glaciers is the formation of supraglacial
38 lakes. These lakes develop when meltwater and precipitation accumulate in topographic
39 depressions formed by heterogeneous glacier thinning in the lower and relatively flat areas of the
40 ablation zone (Echelmeyer et al. 1991; Gibson et al. 2017; Yao et al. 2018). Their formation is
41 accelerated by inefficient drainage of meltwater and the collapse of englacial conduits, leading to
42 localized glacier thinning (Sakai et al. 2000; Huo et al. 2021). Supraglacial lakes are dynamic,
43 ranging in size from a few square meters to tens of square kilometers (Miles et al. 2017). Most
44 lakes drain rapidly if they are linked to the drainage network of the glacier, while some can persist
45 for several years (Qiao et al. 2015; Miles et al. 2017; Wendleder et al. 2021). Some supraglacial

46 ponds and lakes may eventually coalesce and develop into large, moraine-dammed glacial lakes
47 (Richardson and Reynolds 2000; Sakai et al. 2009; Agarwal et al. 2023).

48 Supraglacial lakes significantly affect glacier melt rates, creating a positive feedback loop between
49 surface ablation and lake formation (Thompson et al. 2016; Miles et al. 2019). Due to their lower
50 surface albedo and enhanced convection compared to thick debris, supraglacial lakes amplify
51 glacier melt, particularly at their margins and bottoms, through efficient heat transfer (Benn et al.
52 2001; Xin et al. 2012; Zhu et al. 2024). Consequently, the omission of supraglacial lakes and ponds
53 in the parameterization of glacier mass balance models may lead to an underestimation of melt
54 rates (Huo 2021; Zhu et al. 2024). Furthermore, these lakes play a crucial role in glacier hydrology
55 by regulating the storage and drainage of meltwater (Benn and Evans 2014). Their sudden drainage
56 can deliver large volumes of meltwater to the glacier bed, raising basal water pressure, reducing
57 friction, and ultimately accelerating ice flow or triggering glacier surges (Chudley et al. 2019;
58 Wang and Sugiyama 2024). Rapid drainage events can also generate glacial lake outburst floods
59 (GLOFs), or even trigger secondary GLOFs from downstream lakes by rapidly increasing water
60 levels, for example, the Lemthang Tsho GLOF in 2015 (Gurung et al. 2017). GLOFs originating
61 from supraglacial lakes tend to be smaller in magnitude than those from moraine-dammed lakes,
62 however, they occur more frequently due to the seasonal formation and drainage of supraglacial
63 lakes and can cause extensive destruction (Watson et al. 2018; Miles et al. 2018).

64 A detailed understanding of supraglacial lake evolution is vital for a comprehensive assessment of
65 glacier hydrology and melt dynamics. In the Karakoram, a few studies have examined the long-
66 term evolution and seasonal dynamics of supraglacial lakes (Veetil et al. 2016; Wendleder et al.
67 2018; Wendleder et al. 2021; Qureshi et al. 2023). However, these studies typically focus on
68 specific glaciers, such as Baltoro and Hispar, or do not include the assessment of seasonal

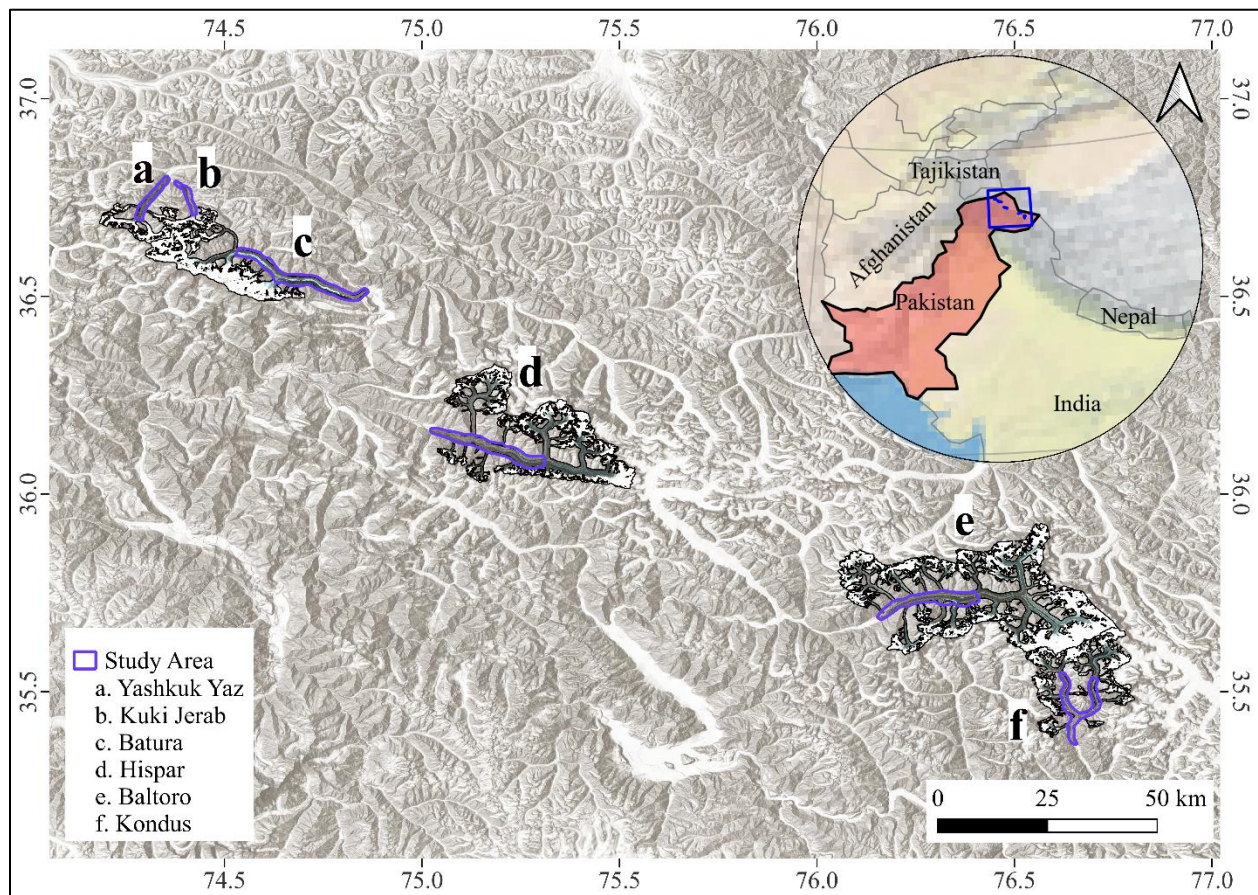
69 supraglacial lake dynamics. Many supraglacial lakes are also missing from regional and global
70 glacial lake inventories due to their small sizes and rapidly changing nature. Observation and
71 continuous monitoring of supraglacial lakes and their evolution in the Karakoram-Himalayas is
72 limited by the absence of hydraulic gaging stations and the frequent clouds brought by the Indian
73 Monsoon during summer, when lake formation is most prevalent (Watson et al. 2016; Miles et al.
74 2018).

75 This study focuses on a comprehensive multi-year assessment of the seasonal dynamics of
76 supraglacial lakes on six glaciers in the Karakoram region, utilizing Sentinel-1 synthetic aperture
77 radar (SAR) data. SAR collects imagery in all weather conditions, providing a consistent dataset
78 essential for analyzing lake dynamics across extensive spatiotemporal scales (Bovenga 2020;
79 Wangchuk and Bolch 2020). The aim of this research is to evaluate the seasonal evolution of
80 supraglacial lakes, investigate their interannual dynamics, and identify the key factors that
81 influence their formation and seasonal fluctuations. To achieve this, we develop monthly lake
82 datasets from May to September over a seven-year period (2017 to 2023) for six debris-covered
83 glaciers. These datasets are then compared with several ancillary data, such as glacier debris
84 thickness, slope, and velocity, to gain a deeper understanding of the interplay between these factors
85 and supraglacial lake dynamics.

86 2. Study Area

87 In this study, we selected six debris-covered glaciers located in the Karakoram Mountains of
88 northern Pakistan (Figure 1). These glaciers were selected based on the occurrence of a
89 considerable number of supraglacial lakes. The lake dynamics analysis was limited to the debris-
90 covered regions within the lower ablation zones of each glacier to minimize potential

91 complications in mapping the lakes, which could arise from seasonal snow at higher elevations.
 92 Our study areas include some of the largest and longest valley glaciers outside the polar regions,
 93 such as Baltoro, Batura, and Hispar. A summary of the glacier characteristics, sourced from the
 94 RGI Consortium (2017), is provided in Table 1.



95
 96 *Figure 1: Study areas of the selected glaciers in the Karakoram in northern Pakistan.*

97

98 *Table 1: Characteristics of the six glaciers and the study areas*

Glacier	RGI ID	Total Area (km ²)	Study Area (km ²)	Glacier Slope / Study Area Slope (°)	Elevation Range (m)
Yashkuk Yaz	RGI60-14.01670	76.97	22.83	23/12.25	3437-6909
Kuki Jerab	RGI60-14.01964	41.11	13.29	24.3/10.73	3597-6828

Batura	RGI60- 14.02150	311.65	83.91	25/9.97	2595-7725
Hispar	RGI60- 14.04477	495.65	77.79	23.3/13.17	3110-7794
Baltoro	RGI60- 14.06794	809.11	67.52	23.8/11	3385-8569
Kondus	RGI60- 14.07239	256.15	55.53	22.8/12.48	3257-7540

99 The Karakoram exhibits a mid-latitude high-mountain climate that is mostly semi-arid, primarily
100 due to its distance from oceanic moisture sources (Copland et al. 2011; Forsythe et al. 2015;
101 Wendleder et al. 2018). The climate is influenced by three distinct weather systems: the westerlies,
102 the Indian summer monsoon, and the Tibetan Anticyclone (Wake 1989; Hewitt 2005; Bashir et al.
103 2017). Winter and spring receive most of the precipitation, the majority of which is contributed by
104 the westerlies, while the monsoonal incursions bring extensive cloud cover, precipitation, and
105 higher temperatures during the summer (Archer and Fowler 2004; Quincey et al. 2009; Haq et al.
106 2023). The wintertime snowfall, driven by the westerlies, sustains the regional snowpack in the
107 Karakoram (Dimri et al. 2015; Javed et al. 2022). The stable anticyclonic weather conditions
108 occasionally weaken, leading to incursions of the Indian monsoon into the Karakoram, which
109 brings heavy precipitation (Wake 1989; Mayer et al. 2006). Air temperature remains sub-zero for
110 most of the year, rising above freezing only during the summer months (June to August) (Reggiani
111 et al. 2017). The microclimatic conditions of the Karakoram region show substantial variation,
112 primarily driven by its wide altitudinal range. The annual mean temperature averages around 2.6
113 °C, while temperatures in the high mountain zones often remain below freezing throughout the
114 year (Wiltshire 2014; Reggiani et al. 2017; Khan et al. 2020).

115 3. Methods

116 3.1 Data

117 Our primary dataset was derived from Sentinel-1 C-band SAR imagery (5.405 GHz, 5.6 cm),
118 specifically the Ground Range Detected (GRD) collection available in Google Earth Engine
119 (GEE). We used the vertical transmit/vertical receive (VV) polarization and the Interferometric
120 Wide Swath (IW) instrument mode data to delineate supraglacial lakes. Sentinel-2 multispectral
121 imaging (MSI) data was used to create normalized difference water index (NDWI) and normalized
122 difference snow index (NDSI) maps and manually delineated validation datasets. Slope masking
123 and glacier surface slope analysis were performed using digital elevation data from the Shuttle
124 Radar Topography Mission (SRTM) (Farr et al. 2007). The Randolph Glacier Inventory (RGI)
125 glacier outlines were utilized to define the study area polygons (RGI Consortium 2017). Glacier
126 velocity maps and mean glacier velocity time series were created using the ITS_LIVE glacier
127 velocity dataset (Gardner et al. 2022). Additionally, we analyzed debris thickness data from
128 Rounce et al. (2021) to assess debris cover across glaciers.

129 3.2 Glacial Lake Mapping

130 The glacial lake mapping process involved three primary steps: (1) data preprocessing and
131 preparation, (2) lake delineation, and (3) accuracy assessment. These steps are summarized below,
132 while a more comprehensive description of the methodology is provided in Khan et al. (2025).

133 3.2.1 Data Preparation

134 We created monthly supraglacial lake datasets for the months of May to September from 2017 to
135 2023. Sentinel-1 GRD imagery in IW mode with VV polarization was imported into GEE and
136 filtered by date and study area. Radiometric distortions in the data were corrected using the gamma

137 naught normalization approach (Small 2011), while a 3x3 median filter was applied to reduce
138 speckle noise, and a preprocessed SAR dataset was prepared. Further, an NDSI mask was used to
139 filter snow-covered areas, and a slope mask was used to remove regions with slopes greater than
140 20 degrees, which commonly introduce classification errors due to terrain-induced radar scattering.
141 These preprocessing steps significantly improved computational efficiency and reduced
142 misclassifications caused by wet snow and mountain shadows.

143 3.2.2 Glacial Lake Delineation

144 The lake delineation was based on the adaptive thresholding of SAR backscatter. Potential water
145 bodies were initially identified using a lenient SAR backscatter threshold of -12 dB, classifying
146 pixels with backscatter values below this threshold as water. The water mask was vectorized into
147 individual polygons, and key attributes were extracted, including surface area and shape index
148 (perimeter-to-area ratio). We applied a minimum surface area (1,000 m²) and a shape index (0.3)
149 filter to eliminate smaller and highly irregular-shaped non-lake features. The minimum lake area
150 threshold was chosen to balance mapping accuracy with the retention of essential lake information.
151 We then applied an adaptive thresholding method based on the Otsu algorithm to reclassify the
152 filtered polygons and obtain the final lake outlines. Manual inspection was conducted to remove
153 false positives, including wet snow patches, glacial ice, and empty crevasses misclassified as lakes.
154 The final lake polygons, along with associated attributes including surface area, mean elevation,
155 and centroid coordinates, were exported as shapefiles for further analysis.

156 3.2.3 Accuracy Assessment

157 To evaluate the accuracy of the SAR-based supraglacial lake mapping, we manually delineated 70
158 lakes using Sentinel-2 MSI false-color composites. This validation dataset included supraglacial

159 lakes across multiple glaciers and years and served as the reference for validating the lake mapping
 160 approach. We assessed the accuracy using mean absolute error (MAE), mean absolute percentage
 161 error (MAPE), root mean square error (RMSE), and the coefficient of determination (R^2). These
 162 metrics quantify both the magnitude of error and the agreement between SAR-derived and
 163 reference lake areas. The MAE and MAPE were obtained using Equations 1 and 2, respectively.

$$164 \quad MAE = \frac{1}{n} \sum_{i=1}^n |Area_{S2} - Area_{S1}| \quad (1)$$

$$165 \quad MAPE = \frac{100}{n} \sum_{i=1}^n \left| \frac{Area_{S2} - Area_{S1}}{Area_{S2}} \right| \quad (2)$$

166 where n is the number of lakes in the validation dataset, $Area_{S1}$ is the area of each lake obtained
 167 from the Sentinel-1 imagery, and $Area_{S2}$ is the area obtained using manual delineation from
 168 Sentinel-2 optical imagery.

169 **3.3 Seasonal Persistence Analysis of Lake-Covered Areas**

170 We quantified supraglacial lake persistence using a pixel-based approach derived from the monthly
 171 lake outlines. For each glacier, all lake polygons from May to September for each year were
 172 rasterized onto a common 10 m grid. During rasterization, pixels whose center fell within a lake
 173 polygon were assigned a value of 1 (lake-covered) and all other pixels were assigned 0. The five
 174 monthly binary rasters (May-September) were then stacked in chronological order, and for each
 175 pixel we calculated the maximum length of a consecutive run of lake presence, yielding annual
 176 values from 0 to 5 months.

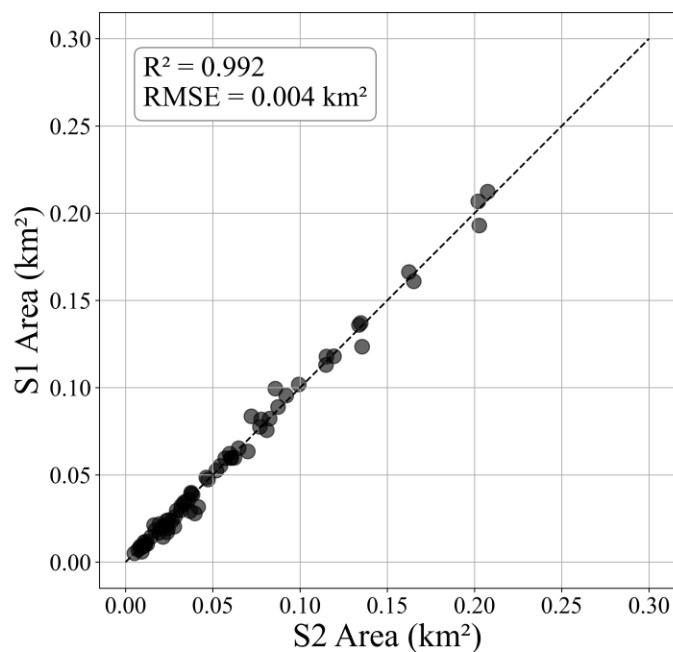
177 We classified pixel-level lake persistence into three categories based on the maximum consecutive
 178 duration: ephemeral (1 month), intermittent (2-3 consecutive months), and persistent (4-5
 179 consecutive months). For each category, lake-covered area was computed by counting the number

180 of pixels assigned to that class and multiplying by pixel area (100 m^2). We then quantified the
 181 relative contribution of each persistence class to the total lake-covered area for each glacier and
 182 year.

183 4. Results

184 4.1 Supraglacial Lake Mapping Accuracy

185 The SAR-derived supraglacial lake
 186 areas showed excellent agreement with
 187 manually delineated lake outlines
 188 derived from Sentinel-2 MSI imagery
 189 (Figure 2). The validation scatterplot
 190 demonstrates a near-one-to-one
 191 relationship between the two datasets
 192 ($R^2 = 0.992$; $\text{RMSE} = 0.004 \text{ km}^2$),
 193 indicating that the SAR-based
 194 delineation reliably captures the lake



195 area across a wide range of sizes. The
 196 overall MAE was 0.003 km^2 , and the

Figure 2: Scatterplot of glacial lake areas derived from Sentinel-1 (S1) SAR and manually digitized Sentinel-2 (S2) imagery. The dashed line is the 1:1 line. The strong agreement ($R^2 = 0.992$, $\text{RMSE} = 0.004 \text{ km}^2$) highlights the accuracy of the SAR-based mapping approach.

197 MAPE was 7.53%, reflecting high mapping accuracy despite the complex surface conditions
 198 typical of debris-covered glaciers.

199 Comparisons of individual lake outlines (Figure S1) further highlight the strong agreement
 200 between the two datasets. In most cases, the SAR-derived boundaries closely matched the optical
 201 reference outlines, with only minor differences along lake edges where radar backscatter

202 transitions gradually into surrounding ice. Larger lakes ($>0.02 \text{ km}^2$) exhibited particularly strong
 203 consistency because their open water surfaces produce distinct low-backscatter signatures that are
 204 easily separable from nearby terrain. Errors were more prominent for very small lakes and those
 205 adjacent to wet snow patches. These conditions reduce the contrast between water and surrounding
 206 surfaces, making it more challenging to distinguish lakes from thin water-saturated snow or
 207 shadowed ice. Nevertheless, these discrepancies were typically small and did not substantially
 208 affect overall lake area estimates. Overall, the validation results confirm that the SAR workflow
 209 provides a robust and reliable method for supraglacial lake mapping across multiple years and
 210 diverse glacier surfaces.

211 4.2 Supraglacial Lake Number and Area Distribution

212 Across the six glaciers, supraglacial lake areas ranged from 0.001 km^2 to 0.50 km^2 , with very few
 213 lakes larger than 0.1 km^2 (Figure 3). The mean number of lakes varied considerably among the
 214 glaciers (Table 2). Kuki Jerab had the lowest mean count (33 lakes), whereas Baltoro had the
 215 highest (223 lakes). The mean lake area ranged from 0.0028 to 0.0062 km^2 , with approximately
 216 70% of the lakes having areas smaller than the mean.

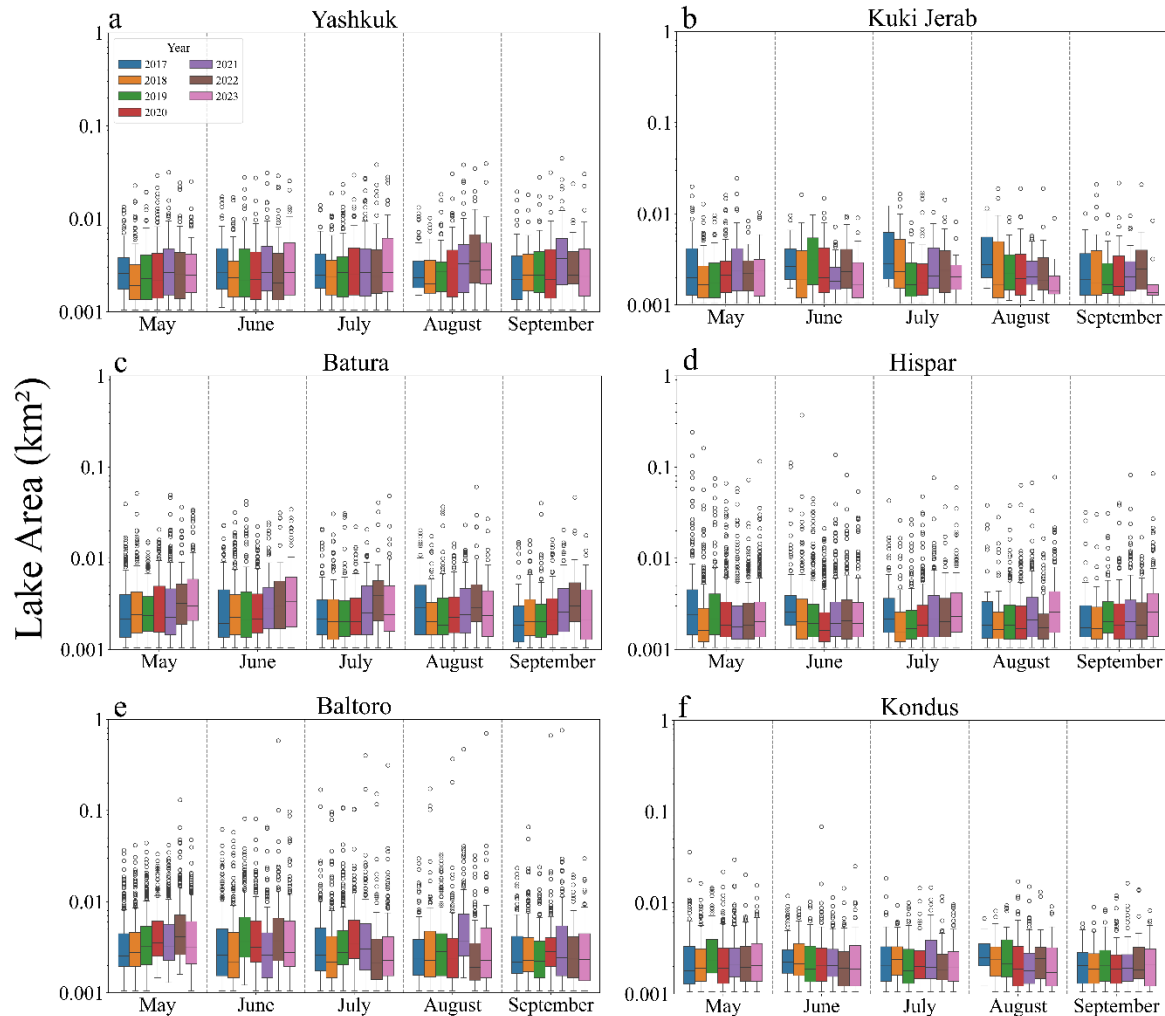
217 Table 2: Summary statistics for each glacier, including the overall minimum, maximum, and mean number of lakes for
 218 each glacier during the study period and the highest, median, and mean lake area for each glacier. The months of the
 219 minimum and maximum lake numbers and maximum area are also shown.

Glacier	Mean Area (km^2)	Max Lake Area (km^2)	Mean No. of Lakes	Min No. of Lakes	Max No. of Lakes	Mean Cumulative Area (km^2)	% of Total Area
Yashkuk Yaz	0.0039	0.0450 (Sep 2021)	76	38 (Aug 2023)	131 (May 2020)	0.293	1.28
Kuki Jerab	0.0031	0.0250 (May 2021)	33	9 (Sep 2023)	87 (May 2018)	0.112	0.84
Batura	0.0039	0.0610 (Aug 2022)	109	46 (July 2022)	223 (May 2021)	0.440	0.52
Hispar	0.0037	0.3700	177	42	404	0.657	0.85

		(June 2018)		(Sep 2017)	(May 2020)		
Baltoro	0.0062	0.5025 (Sep 2021)	223	114 (July 2022)	440 (May 2019)	1.388	2.05
Kondus	0.0028	0.0680 (June 2020)	78	24 (Aug 2022)	272 (May 2020)	0.251	0.45

220 Yashkuk Yaz, Kuki Jerab, Batura, and Kondus were dominated by small lakes, typically < 0.07
 221 km² (Figure 3a-c and f), while Baltoro and Hispar contained lakes larger than 0.1 km² as well
 222 (Figure 3d-e). The cumulative lake area reflected these differences. Baltoro showed the highest
 223 cumulative lake area (2.11 km² in May 2019), followed by Hispar (1.40 km² in May 2017),
 224 whereas the other glaciers had cumulative lake areas that were consistently below 1 km². Lakes
 225 covered between 0.5 and 2% of the study area for each glacier.

226 Seasonal patterns were consistent across all glaciers (Figures 3-4). For each glacier, the peak
 227 number of lakes occurred in May or June, while the fewest were between July and September. The
 228 cumulative lake area and the number of lakes were correlated, both peaking in May or June and
 229 declining as the melt season progressed (Figure 4).

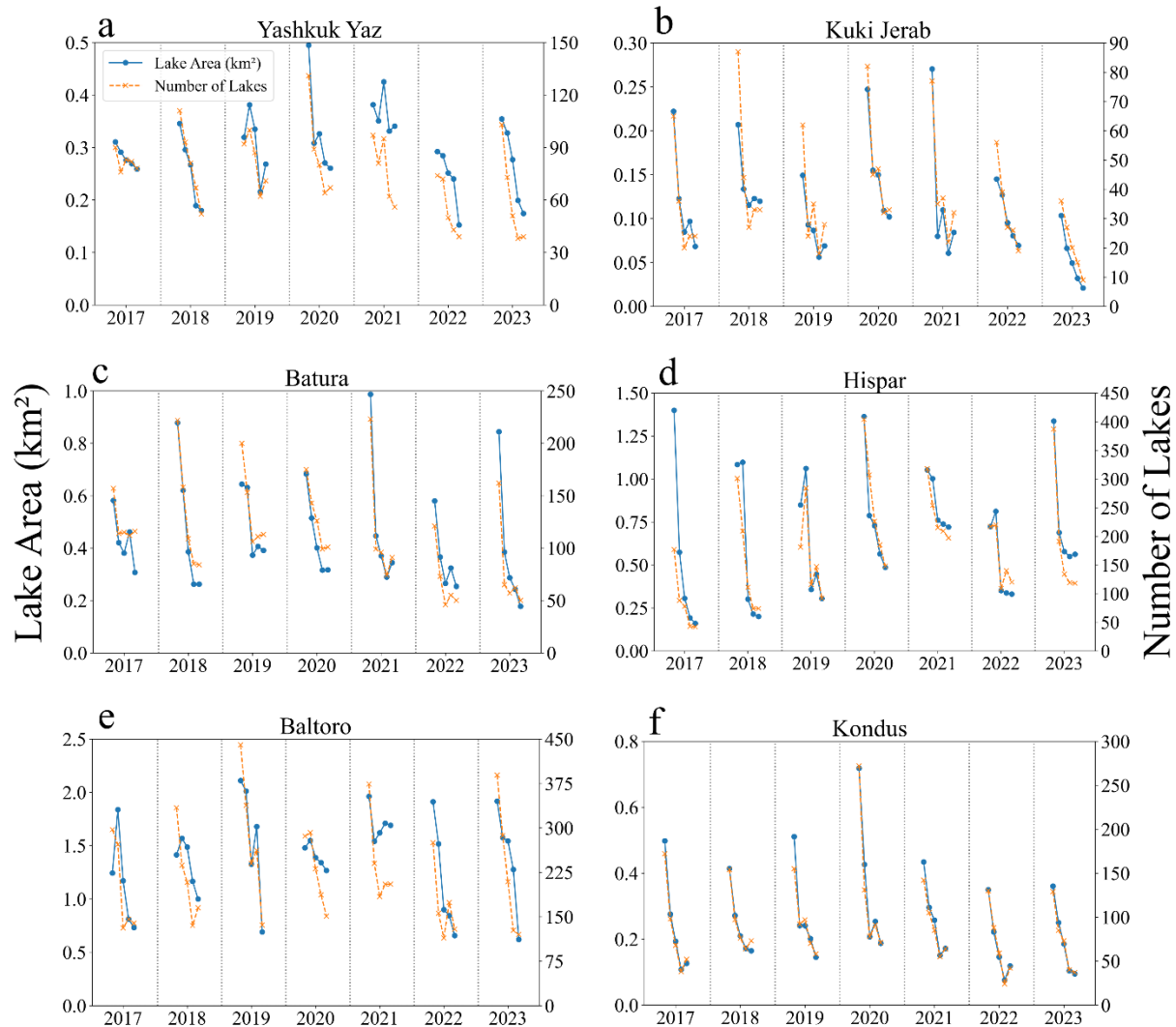


230

231 *Figure 3: Boxplots showing the distribution of supraglacial lake areas for each glacier. The box represents the*
 232 *interquartile range, the central line marks the median, and points beyond the whiskers indicate outliers. Lake areas*
 233 *are plotted on a logarithmic scale to capture the full range of sizes. To compare the lake area dynamics across*
 234 *multiple years, the datasets are grouped by month; for example, all the May datasets from 2017 to 2023 are grouped*
 235 *together.*

236 Interannual variations were also observed. Yashkuk Yaz, Batura, Hispar, and Baltoro showed a
 237 modest increase in median lake area between 2017 and 2023. The most pronounced rise occurred
 238 in August from 2018 to 2022 for Yashkuk Yaz (Figure 3a) and from 2020 to 2023 across all months
 239 for Batura (Figure 3c). Kuki Jerab showed a small increase in the median lake area in May but had
 240 a consistent decline during the peak summer months (Figure 3b), resulting in an overall decreasing
 241 trend. The cumulative lake area did not show any notable change for any glacier, except Kuki

242 Jerab, which had a slightly decreasing trend. Across most glaciers, the highest cumulative lake
 243 areas were observed in May 2020 and 2021. In contrast, 2022 and 2023 exhibited lower cumulative
 244 lake areas, particularly on the Yashkuk Yaz, Kuki Jerab, Batura, and Kondus glaciers (Figure 4).



245

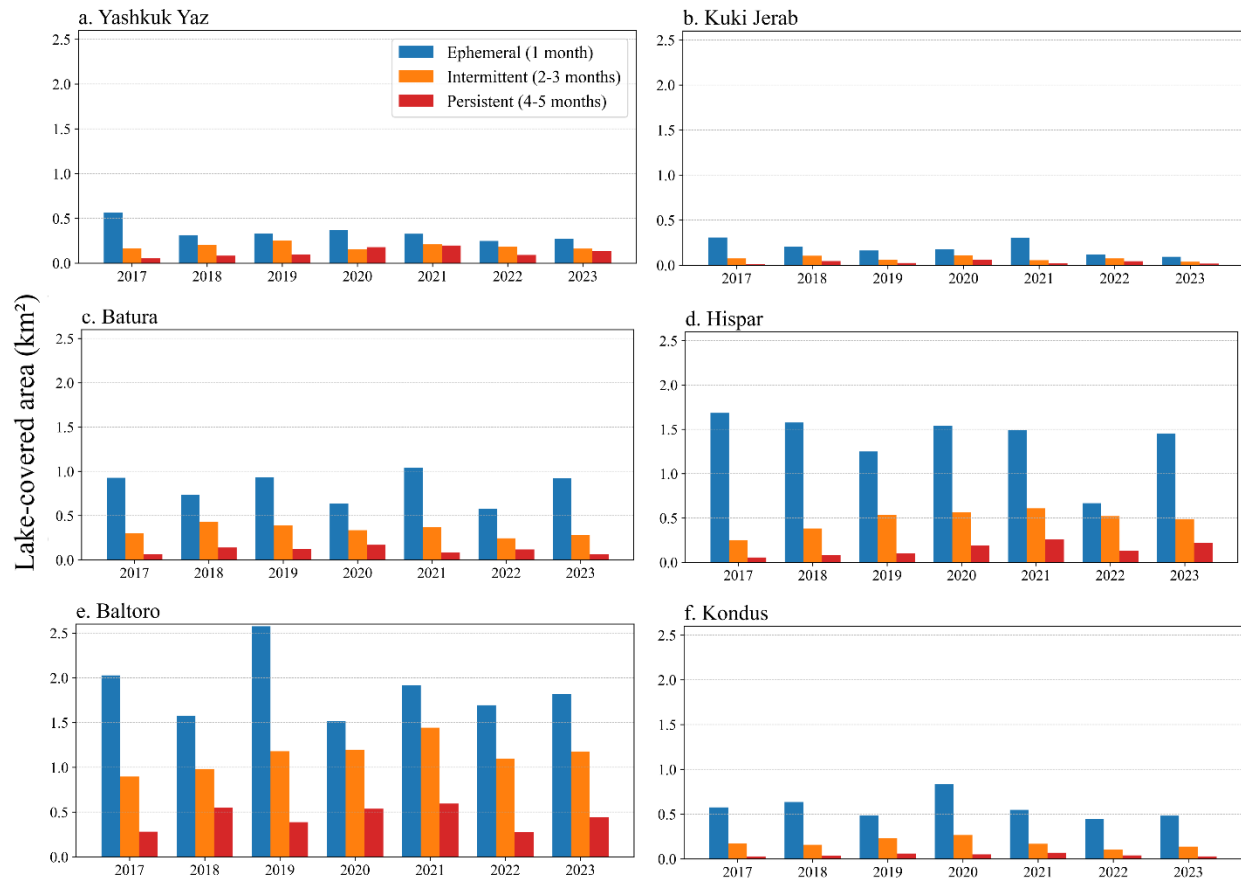
246 *Figure 4: Cumulative monthly lake area and number of lakes from May – September 2017 to 2023 by glacier. The*
 247 *data are plotted as a time series grouped by years to visualize the seasonal evolution of supraglacial lakes, with*
 248 *each dot representing a month, going left to right from May to September. The y-axis scales differ by glacier.*

249 4.3 Seasonal Persistence of Lake-Covered Area

250 Across all six glaciers, supraglacial lake extent persistence during 2017-2023 was consistently
 251 dominated by short-lived inundation of lakes (Figure 5). Ephemeral lake pixels (1 month)

252 represented the largest fraction of total supraglacial lake area on each glacier and in every year,
253 with values ranging from approximately 44-85% across the six glaciers during the study period.
254 Intermittent lake pixels (2-3 months) consistently formed the second-largest class, contributing
255 roughly 13-40% of total lake-covered area. Persistent lake pixels (4-5 months) were present on all
256 glaciers but remained the smallest category, generally comprising 3-26% of lake area throughout
257 the study period.

258 Although the cumulative supraglacial lake area varied among glaciers and across years, the
259 proportional distribution among ephemeral, intermittent, and persistent classes remained broadly
260 consistent within each glacier. No glacier exhibited a clear directional trend in persistence class
261 proportions over the seven-year period, and all sites showed recurrent dominance of short-duration
262 presence or expansion for lakes with a considerably smaller, stable presence of multi-month water
263 pixels.

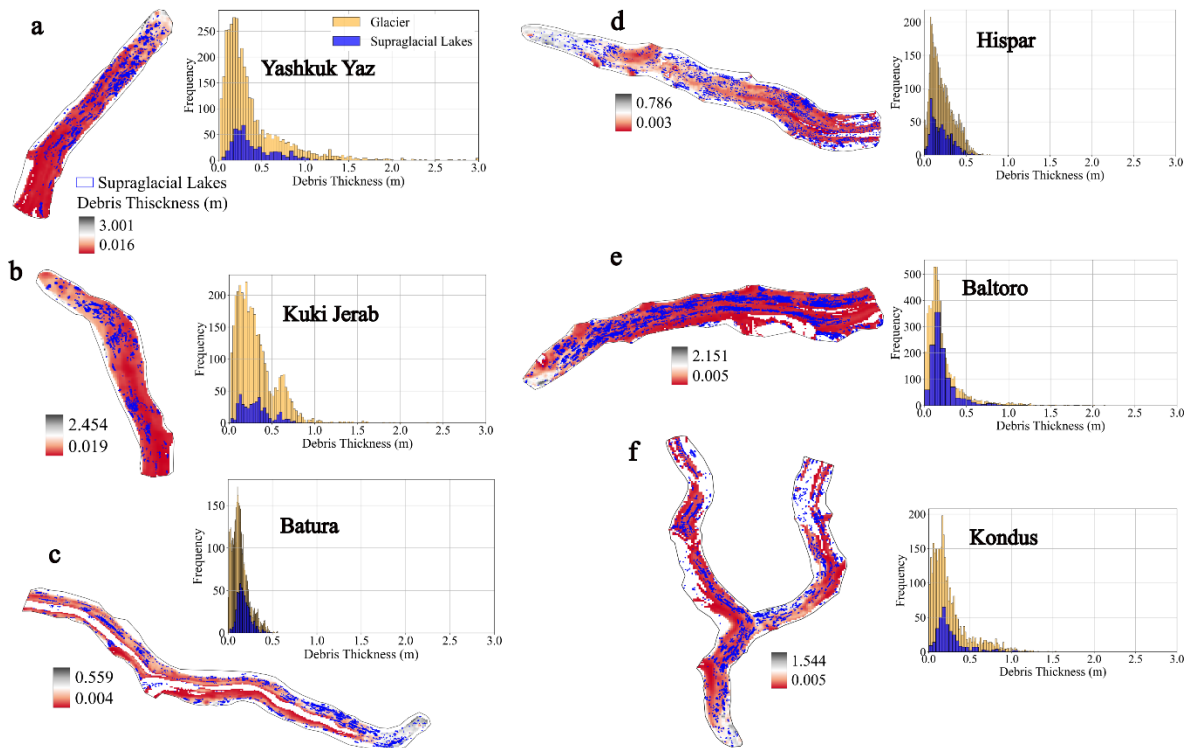


264

265 *Figure 5. Supraglacial lake-covered area persistence across the six glaciers from 2017-2023. The study areas vary*
 266 *widely across the glaciers (Table 1), leading to considerable differences in the histogram bars. Each panel shows*
 267 *the annual supraglacial lake-covered area classified into ephemeral (1 month), intermittent (2-3 months), and*
 268 *persistent (4-5 months) categories based on monthly lake-presence rasters.*

269 4.4 Glacier Characteristics

270 We examined glacier debris thickness, surface slope, and velocity to identify drivers of
 271 supraglacial lake seasonal dynamics. Supraglacial lake formation predominantly occurred in
 272 debris-covered regions (Figure 6). The average debris thickness in the lake-covered areas ranged
 273 from 0.17 m (Batura – Figure 6c) to 0.40 m (Yashkuk Yaz – Figure 6a). Although most lakes
 274 formed where debris thickness was less than 0.5 m, some lakes persisted in areas with debris as
 275 thick as 1.8 m. The thickest debris was observed near the glacier snout, where lake formation was
 276 minimal.



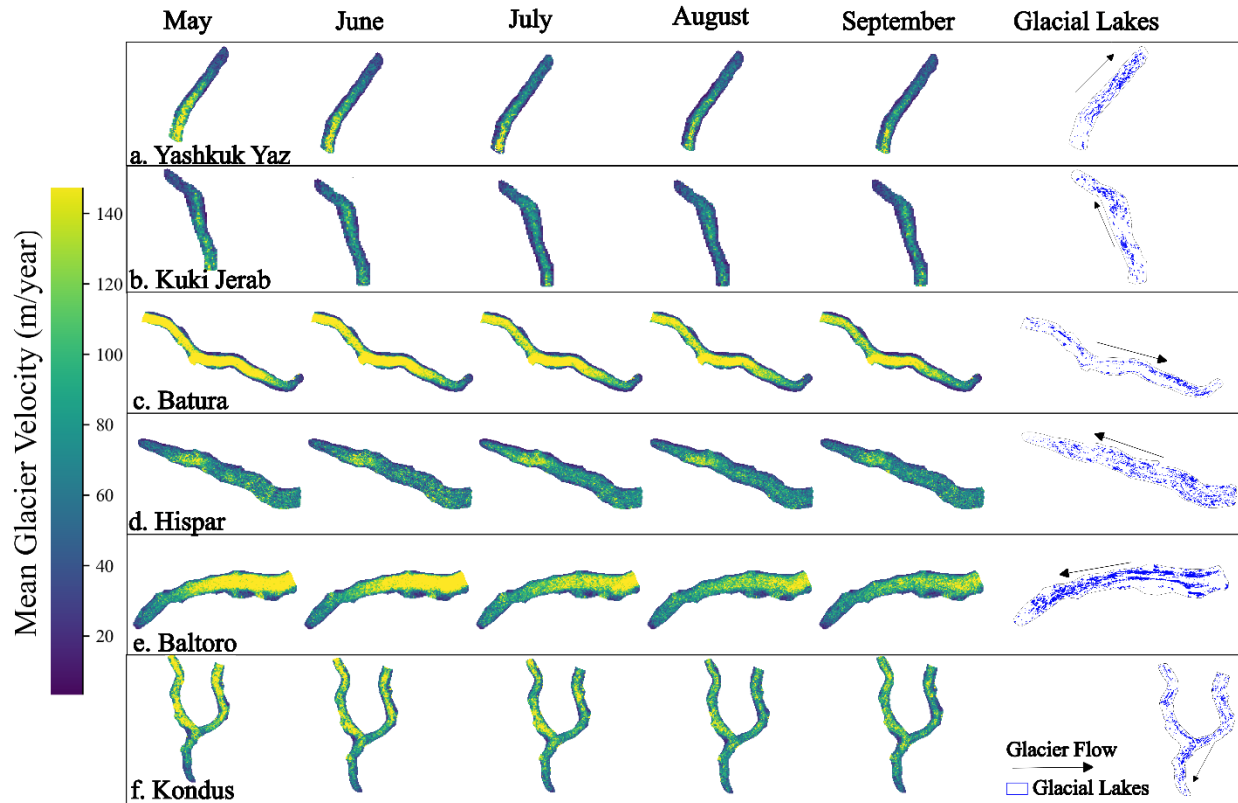
277

278 *Figure 6: Supraglacial lake datasets (2017-2023) overlaid over the debris thickness data obtained from Rounce et*
 279 *al. (2021). The histograms show the debris thickness distribution for the selected glacier area (orange) and the*
 280 *supraglacial lake-covered area (blue).*

281 The majority of lakes were in regions with slopes below 9 degrees. Across the six glaciers, the
 282 mean slope of supraglacial lake-covered areas ranged from 6.0 to 8.9 degrees, which was 2 to 3
 283 degrees flatter than the slopes in areas without lakes.

284 All glaciers exhibited a consistent decrease in surface velocity from May to September, with
 285 velocities also declining toward the glacier snouts. In contrast, higher-elevation regions maintained
 286 relatively greater velocities throughout the melt season. Among the six glaciers, Batura and Baltoro
 287 displayed the highest velocities. Supraglacial lake formation was generally less common in areas
 288 with elevated velocities (Figure 7). This relationship was particularly evident on the Batura Glacier
 289 (Figure 7c), where the central region, characterized by higher velocities, showed an absence of
 290 supraglacial lake development.

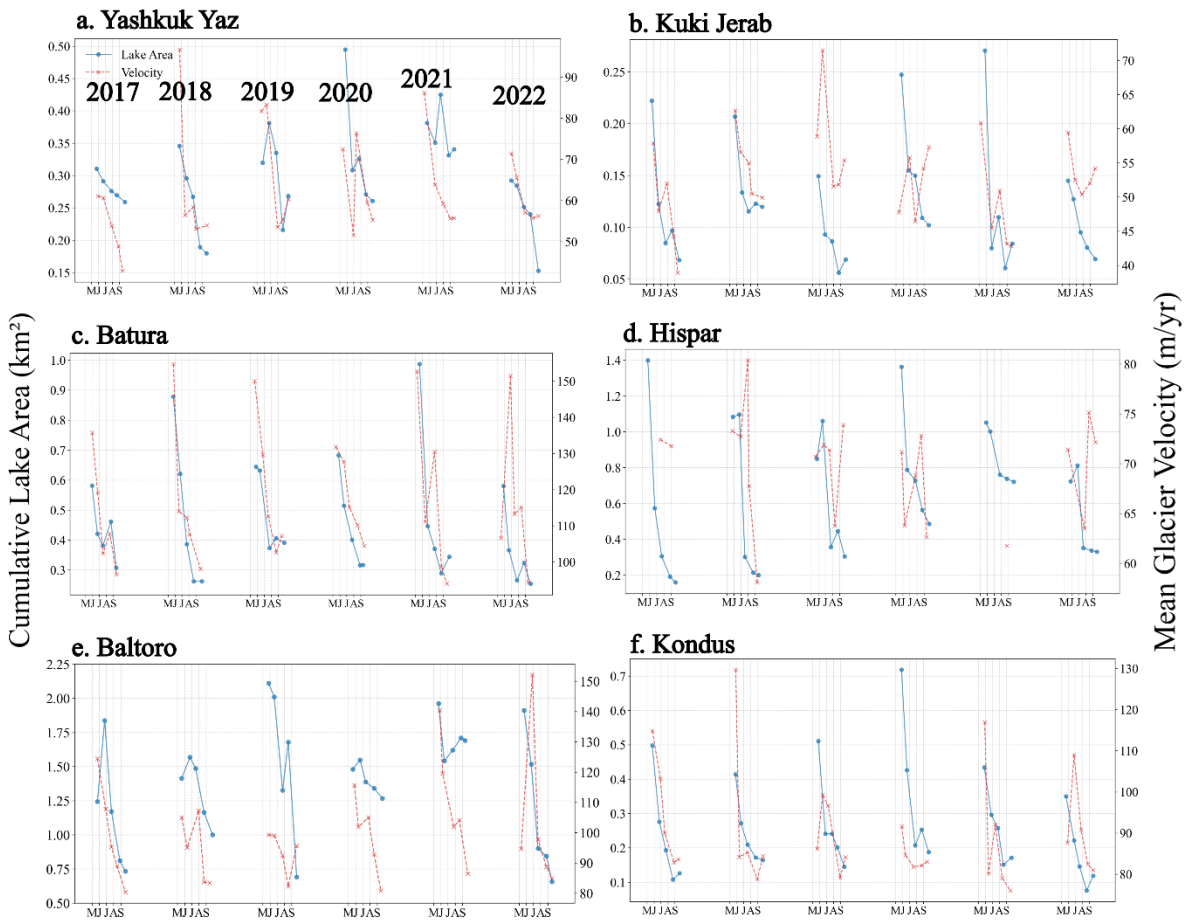
17



291

292 *Figure 7: Monthly mean glacier velocity (m/year) maps for the six glaciers from May to September (2017-2022).*
 293 *Each velocity map represents the average glacier velocity for the corresponding month over the study period. The*
 294 *final column on the right shows the combined glacial lake locations from 2017-2022.*

295 Supraglacial lake formation and subsequent drainage can influence glacier dynamics at broader
 296 spatial and temporal scales. The time series analysis of cumulative lake area and spatially averaged
 297 glacier velocity (Figure 8) shows that periods of high cumulative lake areas (May or June)
 298 coincided with elevated glacier velocities. Statistically significant positive linear correlations were
 299 observed between cumulative lake area and glacier velocity for Yashkuk Yaz ($p = 0.0031$), Batura
 300 ($p = 0.0001$), Baltoro ($p = 0.0459$), and Kondus ($p = 0.0044$). Although Kuki Jerab exhibited an
 301 increase in area with increasing velocity, the correlation was not statistically significant ($p =$
 302 0.1006). In contrast, Hispar ($p = 0.8011$) displayed inconsistent relationships between the lake area
 303 and glacier velocity.



304

305 *Figure 8: Monthly cumulative lake area and spatially averaged glacier velocities (M: May, J: June, J: July, A:*
 306 *August, S: September). These two parameters follow a similar seasonal pattern with some variations, suggesting the*
 307 *role of supraglacial lake drainage in basal sliding. The y-axis scales vary for the plots.*

308 5. Discussion

309 5.1 Supraglacial Lake Dynamics Comparison with Previous Studies

310 Supraglacial lake mapping is challenging due to the smaller size and dynamic nature of the lakes
 311 and complex surroundings (snow, ice, and mountain shadows). As a result, supraglacial lakes are
 312 either completely absent from most global and regional glacial lake inventories or only sparsely
 313 represented (for example, Wang et al. 2020; Shugar et al. 2020). In our study, we used a SAR-
 314 based approach to map supraglacial lakes in the Karakoram. The SAR-based lake mapping

315 facilitated the analysis of seasonal lake dynamics across extensive spatiotemporal scales. Unlike
316 optical imagery, which is often limited by cloud cover and inconsistent availability of useful
317 imagery, the all-weather capability and regular acquisitions of SAR data allowed for the
318 comparison of lake dynamics at uniform temporal intervals.

319 Supraglacial lakes in the Karakoram have been the subject of previous studies. However,
320 comprehensive assessments of seasonal and inter-annual dynamics across multiple glaciers are
321 limited. Wendleder et al. (2018) conducted an analysis of Baltoro's supraglacial lakes from 1991
322 to 2017 using Landsat-8 imagery. Their focus on the long-term evolution of supraglacial lakes
323 provided valuable baseline data. Similarly, Wendleder et al. (2021) used multi-sensor imagery
324 (PlanetScope, Sentinel-2, Sentinel-1, and TerraSAR-X) to assess the seasonal evolution of
325 supraglacial lakes on Baltoro. Qayyum et al. (2020) also mapped Baltoro supraglacial lakes using
326 PlanetScope imagery combined with a deep learning model. The cumulative lake areas obtained
327 in the above studies were slightly higher as compared to our results for Baltoro lakes. These
328 discrepancies were a result of different minimum lake area thresholds and the study area extents.
329 Wendleder et al. (2021) used a threshold of 0.0005 km^2 as opposed to 0.001 km^2 in our study. We
330 mapped the lakes in the lower ablation zone of the main trunk of Baltoro, while these studies
331 considered the whole glacier.

332 The prevalence of small lakes in our study aligns with previous observations of supraglacial lake
333 formation in debris-covered glaciers in various regions in the Karakoram-Himalayas (Mohanty
334 and Maiti 2021; Wendleder et al. 2021; Xu et al. 2023; Zeller et al. 2024). The pronounced
335 seasonality, with peak lake numbers and cumulative area early in the melt season, is also supported
336 by earlier studies in the region (Wendleder et al. 2018; Qayyum et al. 2020; Wendleder et al. 2021).
337 When combining the long-term time series (1991 to 2017) from Wendleder et al. (2018) with our

338 study, a clear increasing trend in lake numbers and cumulative area from 1991 to 2023 is evident,
339 despite our study covering a smaller region. This suggests there is increasing supraglacial lake
340 formation, potentially linked to broader climatic and glaciological factors. Furthermore,
341 Wendleder et al. (2021) reported an increase in the number and area of Baltoro supraglacial lakes
342 larger than 0.01 km^2 , a finding corroborated by our analysis.

343 Beyond Baltoro, few other studies have focused on supraglacial lakes on the region's other
344 glaciers. Qaisar et al. (2018) conducted a Landsat-based analysis of supraglacial lakes on Hispar
345 Glacier using imagery from 1990, 2000, 2010, 2016, and 2017, with each acquisition captured in
346 a different month. In March 2017, they identified 33 lakes. Qureshi et al. (2023) only found 20
347 lakes in 2019. These lake numbers differ considerably compared to our study, where the lowest
348 number of lakes was 42 and 92 in September 2017 and 2019, respectively. This discrepancy may
349 be attributed to differences in the minimum lake area thresholds, which were not explicitly reported
350 in the aforementioned studies. Ashraf and Rustam (2020) mapped supraglacial lakes across the
351 northern region of Pakistan, including the six glaciers in our study. They found 378 supraglacial
352 lakes in the Karakoram in 2013, but did not report lakes by glacier. In our study, the average
353 number of supraglacial lakes over the study period for the six glaciers combined was twice that of
354 Ashraf and Rustam (2020).

355 **5.2 Supraglacial Lake Dynamics in the Karakoram**

356 Our findings highlight that small and ephemeral supraglacial lakes ($<0.01 \text{ km}^2$) dominate the
357 debris-covered glaciers of the Karakoram. The distinct seasonal patterns of lake formation,
358 expansion, and drainage underscore the dynamic nature of supraglacial lakes. The presence of
359 larger and more unstable lakes at higher elevations in May or June, leading to an early-season peak
360 in lake numbers and cumulative area, supports the idea that seasonal snowmelt plays a key role in

361 transient lake formation (Arthur et al. 2020). The subsequent decline in lake number and area later
362 in the season can be attributed to the drainage of the transient lakes as meltwater pathways evolve
363 and efficient englacial drainage systems develop (Qiao et al. 2015; Wendleder et al. 2018).

364 Although lake number and cumulative area generally exhibited a direct correlation, deviations
365 were observed, likely due to the coalescence of smaller lakes into larger ones and the expansion
366 of persistent lakes as the melt season progressed (Leeson et al. 2020; Zeller et al. 2024). This
367 process may explain why some glaciers, for example, Baltoro, experienced an increase in
368 cumulative lake surface area despite an overall decline in the number of lakes.

369 **5.3 Drivers of Supraglacial Lake Formation and Evolution**

370 The pronounced seasonality and fluctuating trends in supraglacial lake dynamics highlight the
371 complex interplay of topographic, glaciological, and meteorological factors in controlling lake
372 formation and persistence (Williamson et al. 2018; Steiner et al. 2019; Wang and Sugiyama 2024).
373 The primary controls on supraglacial lake development are the physical characteristics of the
374 glacier, including debris thickness, glacier velocity, and surface slope, while meteorological
375 conditions play a critical role in their seasonal evolution (Reynolds 2000; Quincey et al. 2007;
376 Dirscherl et al. 2021).

377 **5.3.1 Climatic Drivers**

378 Seasonal temperature fluctuations and precipitation control the timing, extent, and evolution of
379 supraglacial lakes (Qiao et al. 2015; Narama et al. 2017; Wendleder et al. 2021; Dirscherl et al.
380 2021). As spring temperatures rise, increased meltwater availability facilitates the formation and
381 expansion of these lakes, leading to a peak cumulative lake area during May or June. The Indian
382 summer monsoon further amplifies this process by delivering substantial precipitation between

383 May and July (Wendleder et al. 2021). Increased delivery of meltwater to the glacier bed through
384 crevasses and englacial conduits raises basal water pressure, which promotes the development of
385 channelized subglacial drainage networks (Narama et al. 2017; Andrews et al. 2018; Wendleder et
386 al. 2024). This enhanced drainage capacity often triggers the rapid drainage of many supraglacial
387 lakes, leading to a reduction in cumulative lake areas despite sustained high surface temperatures.
388 Some persistent lakes expand and reach maximum sizes later in the summer, either through direct
389 meltwater input or through the coalescence of smaller lakes. For example, Baltoro experienced
390 notable lake expansion during the summer of 2021, contributing to an increase in cumulative lake
391 area. Although climatic conditions control the availability of meltwater, the physical characteristics
392 of the glacier surface govern the supraglacial lakes' spatial distribution.

393 5.3.2 Debris Cover

394 Supraglacial lake formation was predominantly in debris-covered areas, as opposed to debris-free
395 regions. This suggests that debris is a critical factor in supraglacial lake development. Thick and
396 continuous debris reduces glacier melt rates, while thin and patchy debris enhances the melt by
397 increasing the surface albedo (Minora et al. 2015; Fyffe et al. 2019). Consistent with these
398 observations, our study found no supraglacial lake formation in debris-free regions and reduced
399 formation at glacier snouts, where debris thickness was the highest.

400 5.3.3 Glacier Surface Slope

401 In addition to debris, favorable glacier surface slopes and flow velocities are essential for
402 supraglacial lake formation. Gentle slopes and lower surface velocities facilitate meltwater
403 accumulation, thereby promoting supraglacial lake formation (Reynolds 2000; Quincey et al.
404 2007; Miles et al. 2017; Steiner et al. 2019). Our analysis of the six glaciers revealed that the mean
405 slope of lake-covered areas was two to three degrees flatter than that of non-lake areas,

406 corroborating previous research. However, it should be noted that the SRTM DEMs utilized in our
407 analysis are over a decade old and may not represent the current surface gradients of these dynamic
408 Karakoram glaciers. Despite this limitation, our results reinforce the importance of gentle slopes
409 in facilitating the formation of supraglacial lakes.

410 5.3.4 Glacier Velocity

411 A multifaceted relationship exists between glacier velocity and supraglacial lake dynamics. Lower
412 surface velocities promote supraglacial lake formation by maintaining a stable surface that
413 facilitates meltwater accumulation. Higher velocities and the collapse of englacial and sub-glacial
414 conduits can also create surface depressions for lake formation (Gulley and Benn 2007). High
415 glacier velocities may also destabilize existing lakes through surface deformation (Wendleder et
416 al. 2018). Our findings indicate that supraglacial lakes predominantly form in low-velocity regions,
417 as evidenced by their absence in the high-velocity central areas of the Batura and Baltoro glaciers
418 and in high-velocity patches near the snout of the Hispar glacier (Figure 8).

419 Our analysis revealed that spatially averaged glacier velocities and cumulative lake areas are
420 positively correlated. That higher glacier velocities coincide with periods of increased cumulative
421 lake area suggests that the accumulation and subsequent drainage of supraglacial lakes may
422 contribute to seasonal accelerations in glacier flow, as observed for the Baltoro glacier by
423 Wendleder et al. (2024). The volume and timing of meltwater play a critical role in regulating
424 glacier dynamics; meltwater drainage to the glacier bed enhances basal sliding, resulting in
425 temporary accelerations in glacier flow (Glasser 2013; Togaibekov et al. 2024). This relationship
426 is supported by findings from Chudley et al. (2019), who documented a significant increase in
427 glacier surface velocity during a rapid lake drainage event in Greenland. However, supraglacial
428 lake drainage is not the sole contributor to basal meltwater. Meltwater and rainfall delivered

429 through crevasses and subglacial drainage networks may also induce rapid glacier flows during
430 the summer months (Kraaijenbrink et al. 2016; Benn et al. 2017). Therefore, increased glacier
431 velocities can be observed during periods with fewer supraglacial lakes.

432 **6. Conclusion**

433 Our study provides a comprehensive assessment of the seasonal and interannual dynamics of
434 supraglacial lakes in the Karakoram and offers insights into the factors governing lake formation,
435 persistence, and drainage. We found that small supraglacial lakes ($<0.01 \text{ km}^2$) dominate the
436 Karakoram region. There was pronounced seasonality in supraglacial lake formation and
437 evolution, which was consistent over multiple years and across the glaciers. Peak lake numbers
438 and cumulative areas were observed during May or June, while lake drainage dominated later in
439 the season. This trend suggests that rising temperatures in spring influence the formation and
440 expansion of supraglacial lakes. While lake numbers and cumulative areas generally exhibited a
441 positive correlation, deviations from this relationship were observed, likely due to lake
442 coalescence, expansion of persistent lakes, and variable drainage efficiency. Our results further
443 demonstrate that supraglacial lake-covered area is overwhelmingly dominated by short-lived,
444 ephemeral inundation, with small and transient lakes consistently accounting for the majority of
445 seasonal lake extent, while multi-month persistent lakes represent only a minor fraction across
446 glaciers and years.

447 Our analysis identified surface slope, glacier velocity, debris thickness, and climatic conditions as
448 drivers of supraglacial lake formation and evolution. Regions with gentle slopes, lower glacier
449 velocities, and moderate debris thickness had the most lakes. Temporary glacier flow accelerations
450 during lake drainage periods were also observed. The consistency of these patterns across multiple

451 glaciers and the comparative analysis with previous studies suggest that these processes also
452 control supraglacial lake dynamics throughout the Karakoram.

453 This study represents a step forward by quantifying the seasonal dynamics of supraglacial lakes
454 that are largely absent from existing lake inventories. By capturing their consistent seasonal timing,
455 surface controls, and dynamic evolution across multiple glaciers, we provide a more complete
456 picture of glacier surface hydrology in the Karakoram. These findings are important for improving
457 representations of melt processes on debris-covered glaciers, for evaluating the potential for rapid
458 lake drainage and associated hazards, and for assessing how glacier hydrology and downstream
459 water resources may respond to ongoing climate change.

460

461 **Funding**

462 This research was funded by a Fulbright Program grant sponsored by the Bureau of Educational
463 and Cultural Affairs of the United States Department of State and administered by the Institute of
464 International Education.

465 **Data Availability Statement**

466 The original contributions presented in this study are included in the article/Supplementary
467 Material. Further inquiries can be directed to the corresponding author.

468 **Acknowledgments**

469 The authors want to thank Megan Vardaman, Jeremy M. Johnston, and Cameron Wake for
470 providing feedback on the manuscript.

471 **Conflicts of Interest**

472 The authors declare no conflicts of interest. The funders had no role in the design of the study; in
473 the collection, analyses, or interpretation of data; in the writing of the manuscript; or in the decision
474 to publish the results.

475

For Peer Review

476 **References**

- 477 Agarwal, Vibhor, Maximillian Van Wyk de Vries, Umesh K. Haritashya, et al. 2023. “Long-Term
478 Analysis of Glaciers and Glacier Lakes in the Central and Eastern Himalaya.” *Science of The*
479 *Total Environment* 898 (November): 165598. <https://doi.org/10.1016/j.scitotenv.2023.165598>.
- 480 Andrews, Lauren C., Matthew J. Hoffman, Thomas A. Neumann, et al. 2018. “Seasonal
481 Evolution of the Subglacial Hydrologic System Modified by Supraglacial Lake Drainage in
482 Western Greenland.” *Journal of Geophysical Research: Earth Surface* 123 (6): 1479–96.
483 <https://doi.org/10.1029/2017JF004585>.
- 484 Archer, David R., and Hayley J. Fowler. 2004. “Spatial and Temporal Variations in Precipitation
485 in the Upper Indus Basin, Global Teleconnections and Hydrological Implications.” *Hydrology*
486 *and Earth System Sciences* 8 (1): 15.
- 487 Arthur, Jennifer F., Chris R. Stokes, Stewart S. R. Jamieson, J. Rachel Carr, and Amber A.
488 Leeson. 2020. “Distribution and Seasonal Evolution of Supraglacial Lakes on Shackleton Ice
489 Shelf, East Antarctica.” *The Cryosphere* 14 (11): 4103–20. [https://doi.org/10.5194/tc-14-4103-](https://doi.org/10.5194/tc-14-4103-2020)
490 2020.
- 491 Ashraf, Arshad, and Manshad Rustam. 2020. “Monitoring Supraglacial Lakes Formation and
492 Risk of Outburst Flooding in the Himalayan Cryosphere of Pakistan.” *International Journal of*
493 *Environment* 9 (1): 52–67. <https://doi.org/10.3126/ije.v9i1.27587>.
- 494 Bashir, Furrukh, Xubin Zeng, Hoshin Gupta, and Pieter Hazenberg. 2017. “A
495 Hydrometeorological Perspective on the Karakoram Anomaly Using Unique Valley-Based
496 Synoptic Weather Observations.” *Geophysical Research Letters* 44 (20).
497 <https://doi.org/10.1002/2017GL075284>.
- 498 Benn, D. I., S. Wiseman, and K. A. Hands. 2001. “Growth and Drainage of Supraglacial Lakes
499 on Debris-Mantled Ngozumpa Glacier, Khumbu Himal, Nepal.” *Journal of Glaciology* 47 (159):
500 626–38. <https://doi.org/10.3189/172756501781831729>.
- 501 Benn, Douglas, and David J A Evans. 2014. *Glaciers and Glaciation, 2nd Edition*. 0 ed.
502 Routledge. <https://doi.org/10.4324/9780203785010>.
- 503 Benn, Douglas I., Sarah Thompson, Jason Gulle, Jordan Mertes, Adrian Luckman, and Lindsey
504 Nicholson. 2017. “Structure and Evolution of the Drainage System of a Himalayan Debris-
505 Covered Glacier, and Its Relationship with Patterns of Mass Loss.” *The Cryosphere* 11 (5):
506 2247–64. <https://doi.org/10.5194/tc-11-2247-2017>.
- 507 Bisset, Rosie R., Amaury Dehecq, Daniel N. Goldberg, Matthias Huss, Robert G. Bingham, and
508 Noel Gourmelen. 2020. “Reversed Surface-Mass-Balance Gradients on Himalayan Debris-
509 Covered Glaciers Inferred from Remote Sensing.” *Remote Sensing* 12 (10): 1563.
510 <https://doi.org/10.3390/rs12101563>.
- 511 Bovenga, Fabio. 2020. “Special Issue ‘Synthetic Aperture Radar (SAR) Techniques and
512 Applications.’” *Sensors* 20 (7): 1851. <https://doi.org/10.3390/s20071851>.

- 513 Chudley, Thomas R., Poul Christoffersen, Samuel H. Doyle, et al. 2019. "Supraglacial Lake
514 Drainage at a Fast-Flowing Greenlandic Outlet Glacier." *Proceedings of the National Academy
515 of Sciences* 116 (51): 25468–77. <https://doi.org/10.1073/pnas.1913685116>.
- 516 Copland, Luke, Tyler Sylvestre, Michael P. Bishop, et al. 2011. "Expanded and Recently
517 Increased Glacier Surging in the Karakoram." *Arctic, Antarctic, and Alpine Research* 43 (4):
518 503–16. <https://doi.org/10.1657/1938-4246-43.4.503>.
- 519 Dimri, A. P., D. Niyogi, A. P. Barros, et al. 2015. "Western Disturbances: A Review." *Reviews of
520 Geophysics* 53 (2): 225–46. <https://doi.org/10.1002/2014RG000460>.
- 521 Dirscherl, Mariel C., Andreas J. Dietz, and Claudia Kuenzer. 2021. "Seasonal Evolution of
522 Antarctic Supraglacial Lakes in 2015–2021 and Links to Environmental Controls." *The
523 Cryosphere* 15 (11): 5205–26. <https://doi.org/10.5194/tc-15-5205-2021>.
- 524 Echelmeyer, K., T. S. Clarke, and W. D. Harrison. 1991. "Surficial Glaciology of Jakobshavn
525 Isbræ, West Greenland: Part I. Surface Morphology." *Journal of Glaciology* 37 (127): 368–82.
526 <https://doi.org/10.3189/s0022143000005803>.
- 527 Farinotti, Daniel, Walter W. Immerzeel, Remco J. De Kok, Duncan J. Quincey, and Amaury
528 Dehecq. 2020. "Manifestations and Mechanisms of the Karakoram Glacier Anomaly." *Nature
529 Geoscience* 13 (1): 8–16. <https://doi.org/10.1038/s41561-019-0513-5>.
- 530 Farr, Tom G., Paul A. Rosen, Edward Caro, et al. 2007. "The Shuttle Radar Topography
531 Mission." *Reviews of Geophysics* 45 (2): 2005RG000183.
532 <https://doi.org/10.1029/2005RG000183>.
- 533 Forsythe, N., S. Blenkinsop, and H. J. Fowler. 2015. "Exploring Objective Climate
534 Classification for the Himalayan Arc and Adjacent Regions Using Gridded Data Sources." *Earth
535 System Dynamics* 6 (1): 311–26. <https://doi.org/10.5194/esd-6-311-2015>.
- 536 Fyffe, C.L., B.W. Brock, M.P. Kirkbride, et al. 2019. "Do Debris-Covered Glaciers Demonstrate
537 Distinctive Hydrological Behaviour Compared to Clean Glaciers?" *Journal of Hydrology* 570
538 (March): 584–97. <https://doi.org/10.1016/j.jhydrol.2018.12.069>.
- 539 Gardner, Alex, Mark Fahnestock, and Ted Scambos. 2022. "MEaSURES ITS_LIVE Regional
540 Glacier and Ice Sheet Surface Velocities, Version 1." NASA National Snow and Ice Data Center
541 Distributed Active Archive Center. <https://doi.org/10.5067/6II6VW8LLWJ7>.
- 542 Gibson, Morgan J., Neil F. Glasser, Duncan J. Quincey, Christoph Mayer, Ann V. Rowan, and
543 Tristram D.L. Irvine-Fynn. 2017. "Temporal Variations in Supraglacial Debris Distribution on
544 Baltoro Glacier, Karakoram between 2001 and 2012." *Geomorphology* 295 (October): 572–85.
545 <https://doi.org/10.1016/j.geomorph.2017.08.012>.
- 546 Glasser, N.F. 2013. "8.6 Water in Glaciers and Ice Sheets." In *Treatise on Geomorphology*.
547 Elsevier. <https://doi.org/10.1016/B978-0-12-374739-6.00195-0>.

- 548 Gulley, J., and D.I. Benn. 2007. "Structural Control of Englacial Drainage Systems in Himalayan
549 Debris-Covered Glaciers." *Journal of Glaciology* 53 (182): 399–412.
550 <https://doi.org/10.3189/002214307783258378>.
- 551 Gurung, Deo Raj, Narendra Raj Khanal, Samjwal Ratna Bajracharya, et al. 2017. "Lemthang
552 Tsho Glacial Lake Outburst Flood (GLOF) in Bhutan: Cause and Impact." *Geoenvironmental*
553 *Disasters* 4 (1): 17. <https://doi.org/10.1186/s40677-017-0080-2>.
- 554 Haq, Mateeul, Muhammad Jawed Iqbal, Khan Alam, et al. 2023. "Assessment of Runoff
555 Components of River Flow in the Karakoram Mountains, Pakistan, during 1995–2010." *Remote*
556 *Sensing* 15 (2): 399. <https://doi.org/10.3390/rs15020399>.
- 557 Hewitt, Kenneth. 2005. "The Karakoram Anomaly? Glacier Expansion and the 'Elevation Effect,'
558 Karakoram Himalaya." *Mountain Research and Development* 25 (4): 332–40.
- 559 Hewitt, Kenneth. 2011. "Glacier Change, Concentration, and Elevation Effects in the Karakoram
560 Himalaya, Upper Indus Basin." *Mountain Research and Development* 31 (3): 188–200.
561 <https://doi.org/10.1659/MRD-JOURNAL-D-11-00020.1>.
- 562 Huo, Da, Michael P. Bishop, and Andrew B. G. Bush. 2021. "Understanding Complex Debris-
563 Covered Glaciers: Concepts, Issues, and Research Directions." *Frontiers in Earth Science* 9
564 (May): 652279. <https://doi.org/10.3389/feart.2021.652279>.
- 565 Javed, Aaqib, Pankaj Kumar, Kevin I. Hodges, Dmitry V. Sein, Aditya K. Dubey, and Gaurav
566 Tiwari. 2022. "Does the Recent Revival of Western Disturbances Govern the Karakoram
567 Anomaly?" *Journal of Climate* 35 (13): 4383–402. <https://doi.org/10.1175/JCLI-D-21-0129.1>.
- 568 Khan, Adam, Feng Chen, Moinuddin Ahmed, and Muhammad Usama Zafar. 2020. "Rainfall
569 Reconstruction for the Karakoram Region in Pakistan since 1540 CE Reveals Out-of-phase
570 Relationship in Rainfall between the Southern and Northern Slopes of the Hindukush-
571 Karakorum-Western Himalaya Region." *International Journal of Climatology* 40 (1): 52–62.
572 <https://doi.org/10.1002/joc.6193>.
- 573 Khan, Imran, Jennifer M. Jacobs, Jeremy M. Johnston, and Megan Vardaman. 2025. "Mapping
574 Glacial Lakes in the Upper Indus Basin (UIB) Using Synthetic Aperture Radar (SAR) Data."
575 *Glaciers* 2 (4): 13. <https://doi.org/10.3390/glaciers2040013>.
- 576 Kozhikkodan Veetil, Bijeesh, Nilceia Bianchini, Ulisses Franz Bremer, Éder Leandro Bayer
577 Maier, and Jefferson Cardia Simões. 2016. "Recent Variations of Supraglacial Lakes on the
578 Baltoro Glacier in the Central Karakoram Himalaya and Its Possible Teleconnections with the
579 Pacific Decadal Oscillation." *Geocarto International* 31 (1): 109–19.
580 <https://doi.org/10.1080/10106049.2015.1041565>.
- 581 Kraaijenbrink, Philip, Sander W. Meijer, Joseph M. Shea, Francesca Pellicciotti, Steven M. De
582 Jong, and Walter W. Immerzeel. 2016. "Seasonal Surface Velocities of a Himalayan Glacier
583 Derived by Automated Correlation of Unmanned Aerial Vehicle Imagery." *Annals of Glaciology*
584 57 (71): 103–13. <https://doi.org/10.3189/2016AoG71A072>.

- 585 Leeson, A. A., E. Forster, A. Rice, N. Gourmelen, and J. M. Van Wessem. 2020. “Evolution of
586 Supraglacial Lakes on the Larsen B Ice Shelf in the Decades Before It Collapsed.” *Geophysical*
587 *Research Letters* 47 (4): e2019GL085591. <https://doi.org/10.1029/2019GL085591>.
- 588 Mayer, C., A. Lambrecht, M. Belò, C. Smiraglia, and G. Diolaiuti. 2006. “Glaciological
589 Characteristics of the Ablation Zone of Baltoro Glacier, Karakoram, Pakistan.” *Annals of*
590 *Glaciology* 43: 123–31. <https://doi.org/10.3189/172756406781812087>.
- 591 Miles, Evan S., Jakob Steiner, Ian Willis, et al. 2017. “Pond Dynamics and Supraglacial-
592 Englacial Connectivity on Debris-Covered Lirung Glacier, Nepal.” *Frontiers in Earth Science* 5
593 (September): 69. <https://doi.org/10.3389/feart.2017.00069>.
- 594 Miles, Evan S., C. Scott Watson, Fanny Brun, et al. 2018. “Glacial and Geomorphic Effects of a
595 Supraglacial Lake Drainage and Outburst Event, Everest Region, Nepal Himalaya.” *The*
596 *Cryosphere* 12 (12): 3891–905. <https://doi.org/10.5194/tc-12-3891-2018>.
- 597 Miles, Evan S., Ian C. Willis, Neil S. Arnold, Jakob Steiner, and Francesca Pellicciotti. 2017.
598 “Spatial, Seasonal and Interannual Variability of Supraglacial Ponds in the Langtang Valley of
599 Nepal, 1999–2013.” *Journal of Glaciology* 63 (237): 88–105.
600 <https://doi.org/10.1017/jog.2016.120>.
- 601 Miles, Katie E., Bryn Hubbard, Duncan J. Quincey, Evan S. Miles, Tristram D.L. Irvine-Fynn,
602 and Ann V. Rowan. 2019. “Surface and Subsurface Hydrology of Debris-Covered Khumbu
603 Glacier, Nepal, Revealed by Dye Tracing.” *Earth and Planetary Science Letters* 513 (May):
604 176–86. <https://doi.org/10.1016/j.epsl.2019.02.020>.
- 605 Minora, U., A. Senese, D. Bocchiola, et al. 2015. “A Simple Model to Evaluate Ice Melt over the
606 Ablation Area of Glaciers in the Central Karakoram National Park, Pakistan.” *Annals of*
607 *Glaciology* 56 (70): 202–16. <https://doi.org/10.3189/2015AoG70A206>.
- 608 Mohanty, Litan, and Sabyasachi Maiti. 2021. “Probability of Glacial Lake Outburst Flooding in
609 the Himalaya.” *Resources, Environment and Sustainability* 5.
610 <https://doi.org/10.1016/j.resenv.2021.100031>.
- 611 Mölg, Nico, Tobias Bolch, Philipp Rastner, Tazio Strozzi, and Frank Paul. 2018. “A Consistent
612 Glacier Inventory for Karakoram and Pamir Derived from Landsat Data: Distribution of Debris
613 Cover and Mapping Challenges.” *Earth System Science Data* 10 (4): 1807–27.
614 <https://doi.org/10.5194/essd-10-1807-2018>.
- 615 Narama, Chiyuki, Mirlan Daiyrov, Takeo Tadono, et al. 2017. “Seasonal Drainage of
616 Supraglacial Lakes on Debris-Covered Glaciers in the Tien Shan Mountains, Central Asia.”
617 *Geomorphology* 286 (June): 133–42. <https://doi.org/10.1016/j.geomorph.2017.03.002>.
- 618 Qaisar, Maha, Muhammad Shafiq, Badar Munir Khan Ghauri, Isma Younes, and Muhammad
619 Khubaib Abuzar. 2018. *Comparative Analysis of Different Remote Sensing Techniques for*
620 *Mapping of Supraglacial Lakes on Hispar Glacier*. 9 (2): 66–74.

- 621 Qayyum, Nida, Sajid Ghuffar, Hafiz Ahmad, Adeel Yousaf, and Imran Shahid. 2020. “Glacial
622 Lakes Mapping Using Multi Satellite PlanetScope Imagery and Deep Learning.” *ISPRS*
623 *International Journal of Geo-Information* 9 (10): 560. <https://doi.org/10.3390/ijgi9100560>.
- 624 Qiao, Liu, Christoph Mayer, and Shiyin Liu. 2015. “Distribution and Interannual Variability of
625 Supraglacial Lakes on Debris-Covered Glaciers in the Khan Tengri-Tumor Mountains, Central
626 Asia.” *Environmental Research Letters* 10 (1): 014014. <https://doi.org/10.1088/1748-9326/10/1/014014>.
- 628 Quincey, D.J., L. Copland, C. Mayer, M. Bishop, A. Luckman, and M. Belò. 2009. “Ice Velocity
629 and Climate Variations for Baltoro Glacier, Pakistan.” *Journal of Glaciology* 55 (194): 1061–71.
630 <https://doi.org/10.3189/002214309790794913>.
- 631 Quincey, D.J., S.D. Richardson, A. Luckman, et al. 2007. “Early Recognition of Glacial Lake
632 Hazards in the Himalaya Using Remote Sensing Datasets.” *Global and Planetary Change* 56 (1–
633 2): 137–52. <https://doi.org/10.1016/j.gloplacha.2006.07.013>.
- 634 Qureshi, Javed Akhter, Sajid Ali, Garee Khan, Iram Bano, and Shabahat Hussain. 2023. “Inter-
635 Decadal Dynamics of Glacier Area and Supra-Glacial Lakes Over Hispar Glacier, Western
636 Karakoram.” *International Journal of Economic and Environmental Geology* 12 (3): 18–24.
637 <https://doi.org/10.46660/ijeeg.v12i3.57>.
- 638 Reggiani, Paolo, Biswajit Mukhopadhyay, T.H.M. Rientjes, and Asif Khan. 2017. “A Joint
639 Analysis of River Runoff and Meteorological Forcing in the Karakoram, Upper Indus Basin.”
640 *Hydrological Processes* 31 (2): 409–30. <https://doi.org/10.1002/hyp.11038>.
- 641 Reynolds, John. 2000. “On the Formation of Supraglacial Lakes on Debris-Covered Glacier.”
642 *IAHS-AISH Publication* 264 (January): 153–61.
- 643 RGI Consortium. 2017. “Randolph Glacier Inventory - A Dataset of Global Glacier Outlines,
644 Version 6.” National Snow and Ice Data Center. <https://doi.org/10.7265/4M1F-GD79>.
- 645 Richardson, Shaun D, and John M Reynolds. 2000. “An Overview of Glacial Hazards in the
646 Himalayas.” *Quaternary International* 65–66 (April): 31–47. [https://doi.org/10.1016/S1040-6182\(99\)00035-X](https://doi.org/10.1016/S1040-6182(99)00035-X).
- 648 Rounce, D. R., R. Hock, R. W. McNabb, et al. 2021. “Distributed Global Debris Thickness
649 Estimates Reveal Debris Significantly Impacts Glacier Mass Balance.” *Geophysical Research*
650 *Letters* 48 (8): e2020GL091311. <https://doi.org/10.1029/2020GL091311>.
- 651 Sakai, A., K. Nishimura, T. Kadota, and N. Takeuchi. 2009. “Onset of Calving at Supraglacial
652 Lakes on Debris-Covered Glaciers of the Nepal Himalaya.” *Journal of Glaciology* 55 (193):
653 909–17. <https://doi.org/10.3189/002214309790152555>.
- 654 Sakai, Akiko, Nozomu Takeuchi, Koji Fujita, and Masayoshi Nakawo. 2000. *Role of*
655 *Supraglacial Ponds in the Ablation Process of a Debris-Covered Glacier in the Nepal*
656 *Himalayas*. 119–30.

- 657 Shugar, Dan H., Aaron Burr, Umesh K. Haritashya, et al. 2020. “Rapid Worldwide Growth of
658 Glacial Lakes since 1990.” *Nature Climate Change* 10 (10): 939–45.
659 <https://doi.org/10.1038/s41558-020-0855-4>.
- 660 Small, David. 2011. “Flattening Gamma: Radiometric Terrain Correction for SAR Imagery.”
661 *IEEE Transactions on Geoscience and Remote Sensing* 49 (8): 3081–93.
662 <https://doi.org/10.1109/TGRS.2011.2120616>.
- 663 Steiner, Jakob F., Pascal Buri, Evan S. Miles, Silvan Ragettli, and Francesca Pellicciotti. 2019.
664 “Supraglacial Ice Cliffs and Ponds on Debris-Covered Glaciers: Spatio-Temporal Distribution
665 and Characteristics.” *Journal of Glaciology* 65 (252): 617–32.
666 <https://doi.org/10.1017/jog.2019.40>.
- 667 Thompson, Sarah, Douglas I. Benn, Jordan Mertes, and Adrian Luckman. 2016. “Stagnation and
668 Mass Loss on a Himalayan Debris-Covered Glacier: Processes, Patterns and Rates.” *Journal of*
669 *Glaciology* 62 (233): 467–85. <https://doi.org/10.1017/jog.2016.37>.
- 670 Togaibekov, Anuar, Florent Gimbert, Adrien Gilbert, and Andrea Walpersdorf. 2024. “Observing
671 and Modeling Short-Term Changes in Basal Friction During Rain-Induced Speed-Ups on an
672 Alpine Glacier.” *Geophysical Research Letters* 51 (14): e2023GL107999.
673 <https://doi.org/10.1029/2023GL107999>.
- 674 Wake, Cameron P. 1989. “Glaciochemical Investigations as a Tool for Determining the Spatial
675 and Seasonal Variation of Snow Accumulation in the Central Karakoram, Northern Pakistan.”
676 *Annals of Glaciology* 13: 279–84. <https://doi.org/10.3189/s0260305500008053>.
- 677 Wang, Xin, Xiaoyu Guo, Chengde Yang, et al. 2020. “Glacial Lake Inventory of High-Mountain
678 Asia in 1990 and 2018 Derived from Landsat Images.” *Earth System Science Data* 12 (3): 2169–
679 82. <https://doi.org/10.5194/essd-12-2169-2020>.
- 680 Wang, Yefan, and Shin Sugiyama. 2024. “Supraglacial Lake Evolution on Tracy and Heilprin
681 Glaciers in Northwestern Greenland from 2014 to 2021.” *Remote Sensing of Environment* 303
682 (March): 114006. <https://doi.org/10.1016/j.rse.2024.114006>.
- 683 Wangchuk, Sonam, and Tobias Bolch. 2020. “Mapping of Glacial Lakes Using Sentinel-1 and
684 Sentinel-2 Data and a Random Forest Classifier: Strengths and Challenges.” *Science of Remote*
685 *Sensing* 2. <https://doi.org/10.1016/j.srs.2020.100008>.
- 686 Watson, C. Scott, Duncan J. Quincey, Jonathan L. Carrivick, and Mark W. Smith. 2016. “The
687 Dynamics of Supraglacial Ponds in the Everest Region, Central Himalaya.” *Global and*
688 *Planetary Change* 142 (July): 14–27. <https://doi.org/10.1016/j.gloplacha.2016.04.008>.
- 689 Watson, Cameron Scott, Duncan J. Quincey, Jonathan L. Carrivick, Mark W. Smith, Ann V.
690 Rowan, and Robert Richardson. 2018. “Heterogeneous Water Storage and Thermal Regime of
691 Supraglacial Ponds on Debris-covered Glaciers.” *Earth Surface Processes and Landforms* 43 (1):
692 229–41. <https://doi.org/10.1002/esp.4236>.

- 693 Wendleder, Anna, Jasmin Bramboeck, Jamie Izzard, et al. 2024. “Velocity Variations and
694 Hydrological Drainage at Baltoro Glacier, Pakistan.” *The Cryosphere* 18 (3): 1085–103.
695 <https://doi.org/10.5194/tc-18-1085-2024>.
- 696 Wendleder, Anna, Peter Friedl, and Christoph Mayer. 2018. “Impacts of Climate and
697 Supraglacial Lakes on the Surface Velocity of Baltoro Glacier from 1992 to 2017.” *Remote
698 Sensing* 10 (11): 1681. <https://doi.org/10.3390/rs10111681>.
- 699 Wendleder, Anna, Andreas Schmitt, Thilo Erbertseder, Pablo D’Angelo, Christoph Mayer, and
700 Matthias H. Braun. 2021. “Seasonal Evolution of Supraglacial Lakes on Baltoro Glacier From
701 2016 to 2020.” *Frontiers in Earth Science* 9 (December): 725394.
702 <https://doi.org/10.3389/feart.2021.725394>.
- 703 Williamson, Andrew G., Ian C. Willis, Neil S. Arnold, and Alison F. Banwell. 2018. “Controls on
704 Rapid Supraglacial Lake Drainage in West Greenland: An Exploratory Data Analysis Approach.”
705 *Journal of Glaciology* 64 (244): 208–26. <https://doi.org/10.1017/jog.2018.8>.
- 706 Wiltshire, A. J. 2014. “Climate Change Implications for the Glaciers of the Hindu Kush,
707 Karakoram and Himalayan Region.” *The Cryosphere* 8 (3): 941–58. <https://doi.org/10.5194/tc-8-941-2014>.
- 709 Xie, Fuming, Shiyin Liu, Yongpeng Gao, et al. 2023. “Interdecadal Glacier Inventories in the
710 Karakoram since the 1990s.” *Earth System Science Data* 15 (2): 847–67.
711 <https://doi.org/10.5194/essd-15-847-2023>.
- 712 Xin, Wang, Liu Shiyin, Han Haidong, Wang Jian, and Liu Qiao. 2012. “Thermal Regime of a
713 Supraglacial Lake on the Debris-Covered Koxkar Glacier, Southwest Tianshan, China.”
714 *Environmental Earth Sciences* 67 (1): 175–83. <https://doi.org/10.1007/s12665-011-1490-1>.
- 715 Xu, Jinhao, Min Feng, Yijie Sui, Dezhao Yan, Kuo Zhang, and Kaidan Shi. 2023. “Identifying
716 Alpine Lakes in the Eastern Himalayas Using Deep Learning.” *Water* 15 (2): 229.
717 <https://doi.org/10.3390/w15020229>.
- 718 Yao, Xiaojun, Shiyin Liu, Lei Han, Meiping Sun, and Linlin Zhao. 2018. “Definition and
719 Classification System of Glacial Lake for Inventory and Hazards Study.” *Journal of
720 Geographical Sciences* 28 (2): 193–205. <https://doi.org/10.1007/s11442-018-1467-z>.
- 721 Zeller, Lucas, Daniel McGrath, Scott W. McCoy, and Jonathan Jacquet. 2024. “Seasonal to
722 Decadal Dynamics of Supraglacial Lakes on Debris-Covered Glaciers in the Khumbu Region,
723 Nepal.” *The Cryosphere* 18 (2): 525–41. <https://doi.org/10.5194/tc-18-525-2024>.
- 724 Zhu, Yu, Shiyin Liu, Ben W. Brock, et al. 2024. “Debris Cover Effects on Energy and Mass
725 Balance of Batura Glacier in the Karakoram over the Past 20 Years.” *Hydrology and Earth
726 System Sciences* 28 (9): 2023–45. <https://doi.org/10.5194/hess-28-2023-2024>.
- 727